land

MDPI

Article

Impacts of Future Sea-Level Rise under Global Warming Assessed from Tide Gauge Records: A Case Study of the East Coast Economic Region of Peninsular Malaysia

Milad Bagheri [1], Zelina Z. Ibrahim [2], Mohd Fadzil Akhir [1], Bahareh Oryani [3], Shahabaldin Rezania [4], Isabelle D. Wolf [5,6], Amin Beiranvand Pour [1] and Wan Izatul Asma Wan Talaat [1,*]

1 Institute of Oceanography and Environment, Universiti Malaysia Terengganu, Kuala Nerus 21030, Malaysia; milad.bagheri.gh@umt.edu.my (M.B.); mfadzil@umt.edu.my (M.F.A.); beiranvand.pour@umt.edu.my (A.B.P.)
2 Department of Environment, Faculty of Environmental and Forestry, Universiti Putra Malaysia, Seri Kembangan 43400, Malaysia; zelina@upm.edu.my
3 Technology Management, Economics and Policy Program, College of Engineering, Seoul National University, 1 Gwanak-ro, Gwanak-gu, Seoul 08826, Korea; bahare.oryani@snu.ac.kr
4 Department of Environment and Energy, Sejong University, Seoul 05006, Korea; shahab.rezania@sejong.ac.kr
5 School of Geography and Sustainable Communities, University of Wollongong, Northfields Avenue, Wollongong, NSW 2522, Australia; iwolf@uow.edu.au
6 Centre for Ecosystem Science, University of New South Wales, Sydney, NSW 2052, Australia
* Correspondence: wia@umt.edu.my

Citation: Bagheri, M.; Ibrahim, Z.Z.; Akhir, M.F.; Oryani, B.; Rezania, S.; Wolf, I.D.; Pour, A.B.; Talaat, W.I.A.W. Impacts of Future Sea-Level Rise under Global Warming Assessed from Tide Gauge Records: A Case Study of the East Coast Economic Region of Peninsular Malaysia. *Land* **2021**, *10*, 1382. https://doi.org/10.3390/land10121382

Academic Editor: Isa Ebtehaj

Received: 9 November 2021
Accepted: 6 December 2021
Published: 14 December 2021

Abstract: The effects of global warming are putting the world's coasts at risk. Coastal planners need relatively accurate projections of the rate of sea-level rise and its possible consequences, such as extreme sea-level changes, flooding, and coastal erosion. The east coast of Peninsular Malaysia is vulnerable to sea-level change. The purpose of this study is to present an Artificial Neural Network (ANN) model to analyse sea-level change based on observed data of tide gauge, rainfall, sea level pressure, sea surface temperature, and wind. A Feed-forward Neural Network (FNN) approach was used on observed data from 1991 to 2012 to simulate and predict the sea level change until 2020 from five tide gauge stations in Kuala Terengganu along the East Coast of Malaysia. From 1991 to 2020, predictions estimate that sea level would increase at a pace of roughly 4.60 mm/year on average, with a rate of 2.05 ± 7.16 mm on the East Coast of Peninsular Malaysia. This study shows that Peninsular Malaysia's East Coast is vulnerable to sea-level rise, particularly at Kula Terengganu, Terengganu state, with a rate of 1.38 ± 7.59 mm/year, and Tanjung Gelang, Pahang state, with a rate of 1.87 ± 7.33 mm/year. As a result, strategies and planning for long-term adaptation are needed to control potential consequences. Our research provides crucial information for decision-makers seeking to protect coastal cities from the risks of rising sea levels.

Keywords: feed-forward model; tide gauge; sea-level residual; time series analysis; coastal city vulnerability

1. Introduction

Because the human population in coastal areas is growing, nearly 70% of the world's beaches are retreating. Only 20% of the region is regarded as stable, while the other 10% is considered to be in a state of retreat [1,2]. More than 200 million people living within one meter of the mean sea level will be most directly affected by changes in the Global Sea Level (GSL) [3–5]. Climate change and global warming are a threat to the environment as well as the environment's primary users, most people. As the earth warms due to rising temperatures, the latter occurs [6]. Natural processes such as heavy rainfall, sea-level rise, erosion, flood, and human activity constantly affect the structure and morphologic characteristics of coastal city zones [7].

Sea-level rise is one of the most devastating effects of global climate change that will have far-reaching consequences for the majority of the world's population and ecosystems [8]. General Circulation Models (GCMs) estimate that the GSL is increasing, possibly at an accelerated rate [9] due to the delayed effect of the divergence of the climate change estimates arising from the time-integrating feature of the sea level [10]. For the last 100 years, the best estimate for the rate of the global mean sea-level rise is 1.05 mm/year [11]. From 1985 to 2030, the predictions for the mean sea-level rise range from 8–29 cm, while they range from 21–71 cm from 1985 to 2070. These estimates will largely be influenced by the thermal expansion of oceans and the increased melting of mountain glaciers and small ice caps [12].

Malaysia is classified as a country that faces a moderate risk from climate change. Severe climate-change-related disasters such as floods, storms, and droughts have occurred in Pahang, Johor, Kelantan, Kedah, and Terengganu. This foreshadows likely adverse impacts and threats to Malaysia in the future [13]. Several important studies have been conducted by the National Hydraulic Research Institute of Malaysia (NAHRIM) regarding imminent climate change issues relating to projected sea-level rises, production of inundation maps, and coastal vulnerability assessments of high-risk areas [14].

Sea level change will affect marine habitats and ecosystems along with natural coastal processes with likely impacts on infrastructure and the socio-economy. This impedes the development and conservation of coastal cities [15]. Knowledge is needed to prepare for and alleviate this hazard. In this research, we develop an Artificial Neural Network (ANN) model to analyse and predict sea-level change in the vulnerable area of Kuala Terengganu. Output from this study will be vital for the establishment of policies for the East Coast Economy Region (ECER), a government initiative to enhance the socio-economy of the Malaysian East Coast region [16].

One of the most important devices and measures of sea-level change is the tide gauge. It measures the height of the water level periodically for a height reference surface that can be physically defined from the water level [17] to generate a continuous sea-level time sequence [18–20]. This type of measurement to assess water depth dates back to the 17th century [21]. A tide gauge typically measures tides, effects of ocean circulation, meteorological water forces, local or regional uplift or subsidence at the measurement site, and gauge-inherent errors [22]. Also determined by tidal observation is the typical behavior of water levels during abrupt climate change events such as El-Niño/La Nina and the Northeast Monsoon [23]. There are five tidal stations located along the East Coast of Malaysia. Figure 1 presents an overview of the tide gauge measurement systems, including their names and dates of establishment. In Malaysia, each tide gauge station consists of protective housing for the tide gauge, stilling or tide well; tide staff, and numerous reference benchmarks, one of which is known as the tide gauge benchmark [24]. The most commonly used floating, tide gauge measuring device operates in a stilling well (Figure 1).

Analyzing tide gauge data to predict sea-level rise is common practice in coastal city studies [25]. However, alternative mesh-less artificial intelligence methods, namely fuzzy logic, genetic algorithms, or ANNs could be utilized to resolve the issues entailed in near-shore sea-level predictions, as we discuss in the following [26]. The initial development of ANNs occurred in the 1940s, though the development experienced a resurgence, especially with the efforts of iterative auto-associable neural networks [27]. In recent decades, ANNs are widely applied because of refined algorithms, which help overcome several limitations discovered in the early networks [28]. The fields of application are extensive, including environmental modeling, geosciences, data validation, and risk management [29–31]. ANNs overcome the difficulties of the new nonlinear statistical approaches used among geosystem elements [32–35]. Compared to other standard statistical methods, neural networks have the advantage of automatically permitting indiscriminate nonlinear relationships between dependent and independent variables as well as all potential interactions between the dependent variables.

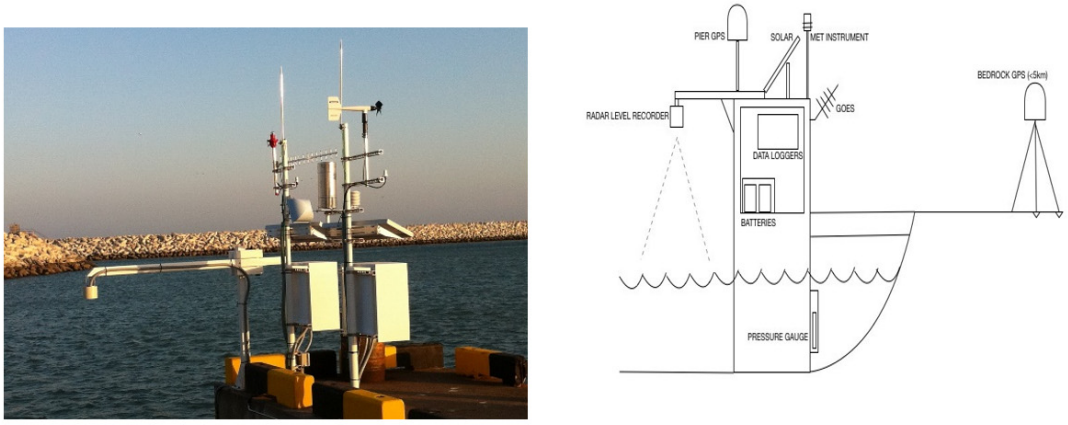

Tidal station	Location		Established Date	Type of Tide Gauge Used
	Latitude	Longitude		
Juhor Bahru	1 27 42 N	103 47 30 E	Dec. 1983	Kyowa Shoko LTT-3AD
Tioman	2 48 26 N	104 08 24 E	Nov. 1985	Kyowa Shoko LTT-3AD
Tanjung Gelang	2 12 54 N	102 9 12 E	Dec. 1983	Kyowa Shoko LTT-3AD
Cendering	5 15 54 N	103 11 12 E	Oct. 1984	Kyowa Shoko LTT-3AD
Geting	6 13 35 N	102 06 24 E	Oct. 1986	Kyowa Shoko LTT-3AD

Figure 1. Schematic of a tide gauge measurement system and locations and details of stations based in Terengganu, along the East Coast of Peninsular Malaysia. Source: the pictures from https://www.sutron.com/product/tide-stations/, accessed on 1 December 2021, and https://www.unavco.org/instrumentation/geophysical/tide-gauges/tide-gauges.html, accessed on 1 December 2021.

In contrast, standard statistical methods need supplementary modeling to accommodate for this flexibility. Moreover, ANNs do not require obvious distributional assumptions [36,37]. ANNs that can estimate nonlinear mathematical functions [38] permit possible simulations of complex systems behavior without prior knowledge of the internal relationships among their constituents [39].

The ability to generalize constitutes another major advantage of neural networks. ANN models can learn to perform a specific task based on available empirical data. Such models integrate an innovative information processing system structure. In essence, the distinctive advantage of ANNs relative to other methods is the self-learning capacity that equips them to specify the essential connection between input and output variables without prior knowledge of the nature of the association. This makes ANNs suitable for solving complex nonlinear problems that cannot be resolved analytically, according to [40–42]. ANN models are therefore superior to other traditional statistical models such as Multiple Linear Regression (MLR) models, which are not appropriate for non-normally distributed data [43]. ANNs also can resolve specific problems. ANN models are organized in a great number of interconnected processing neurons or nodes that work in unity as powerful tools for modeling [44]. ANN models work as a black box and function without comprehensive system information because they use historical data to study the connection between input and output parameters. ANNs can train themselves from diverse samples via learning algorithms. Every time an ANN is generalized, it is capable of uniting the input data in proper precision irrespective of whether they utilized them in the learning stages [45]. The weights in the ANN are adjustable and can interrelate and react to its setting. Therefore, ANNs react adequately to situational changes and continue to train themselves after the original training session [46]. ANNs could be described as estimators of semi-parametric regression. Hence, they can access virtually any (measurable) function to an indiscriminate amount of accuracy [47].

Neural networks might have a special appeal due to their apparent similarity to the human brain. They appear to provide "prediction" without the problems connected to the

utilization of mathematics. Ref. [48] noted that the challenge in developing ANN models is the absence of set methods to construct the network architecture. In this study, we have applied the most popular kind of ANNs, namely the feed-forward back-propagation multi-perceptron hierarchical architecture. The Feed-Forward Neural Network (FNN) possesses a distributed and parallel processing structure. It consists of three layers, namely an input layer (to enter data into the network); an output layer (to create a suitable response to the specified input); and one or more intermediate layers, where the training algorithm repeatedly modifies the connection weights (synapses) which store the knowledge required to solve particular problems [49,50]. The multi-layered FNN can forecast hourly temperatures 24 h in advance with sufficient accuracy [51]. Back-propagation is a learning device that resolves predictions in multilayer perceptron networks and requires differentiability in the output layers activation function, according to [52].

The literature relating to meteorology and coastal management reveals that:

1. While ANNs have been studied and widely adopted on a large scale, FNN applications are scarce, especially for sea-level predictions.
2. FNN models are mostly used because of their efficacy.
3. FNN models are superior to other ANN models in terms of their simulation and prediction.

Using data on sea-level residual, tide gauge, rainfall, sea level pressure, sea surface temperature, and wind (from climate re-analysis) and other measures, several types of research have been published on forecasting sea level by its non-astronomical component, that is, monthly tide gauge. Therefore, the FNN and other ANN models can be investigated to increase the accuracy of the simulation and estimation of seawater levels by tide gauge anomalies.

The general objective of this study is to improve the management and planning of vulnerable areas along the East Coast of Peninsular Malaysia. The two specific objectives of the present work are: (1) To investigate the extent to which the precision of the simulation and predictions of the sea level can be improved by harnessing local knowledge on climate at various locations. (2) To compare the simulation and prediction effects of five tide gauge stations using an FNN model on the east coast of Peninsular Malaysia.

2. Material and Methods

2.1. Study Site

Because it is part of Peninsular Malaysia's East Coast Economic Region (ECER), which includes four states: Kelantan, Terengganu, and Pahang, as well as the district of Mersing in northeast Johor, five tidal gauge stations, were chosen as a study area [53] (Figure 2). The first tidal gauge station (Johor Bahru) is located between the latitudes of 01°27.7″ N and the longitudes of 103°47.5″ E in the Jeti Kastam Johor Bahru. The Tidal Station's Zero of Tide Gauge is 6.079 m below survey department brass BM J0416 or 2.657 m below DTGSM. Johor Bahru is a city in Malaysia. The value of 7.034 m was achieved in May of 1998. The second tidal gauge station (Pulau Tioman) is located between the latitudes of 02°48.4″ N and the longitudes of 104°08.4″ E in the Jeti Berjaya Kuantan. The established value for Pulau Tioman is 7.930 m, and it was established in May of 1998. At Tidal Station, the zero of the tide gauge is 6.586 m below survey department brass BM C0501. Monsoon winds and tides, in essence, are essential natural factors that help shape the Kuantan Coastline. Due to its location as an active tourism gateway to the East Coast Economic Region, Pulau Tioman station was chosen as the fourth tidal gauge station. There are various unique tourism attractions, particularly in the fields of mainland coastal and sustainable island tourism, ecotourism, urban tourism, and the country's traditional culture and heritage tourism. The third tidal gauge station (Tanjung Gelang) is situated between 03°58.5″ N and 103°11.2″ E in Pelabuhan Kuantan. At the tidal station, the zero of the tide gauge is 6.496 m below survey department brass BM C0331 or 2.661 m below DTGSM. The Tanjung Gelang date of establishment is April 1998, and the established value is 7.731 m. The fourth tide gauge station (Cendering) is located in the eastern part of Terengganu, near the coastal city of Kuala Terengganu, which is also the state capital and has a population of 286,317 people.

It is located between latitudes of 05°15.9″ N and longitudes of 103°11.2″ E. Tidal Station's zero is 4.688 m below survey department brass BM T0283 or 2.084 m below DTGSM, and is located on the left corner of the T-junction facing Tidal Station. The Cendering established value is 6.732 m, and the date of establishment is April 1998. With semi-diurnal tides and an average yearly temperature of 25 °C to 27 °C, the northeast monsoon dominates the coast in this area. The fourth tide gauge station (Getting) is located in Kelantan's north, near Kompleks LKIM, between latitudes of 06°13.06″ N and longitudes of 102°06.4″ E, with an established value of 7.230 m and data from April 1998. At Tidal Station, the zero of the tide gauge is 5.964 m below survey department brass BM D0354 or 2.112 m below DTGSM. In Pahang, Johor, Kelantan, Kedah, and Terengganu, severe weather phenomena such as floods, storms, droughts, and climate patterns have occurred. These occurrences show that Malaysia is vulnerable to climate change.

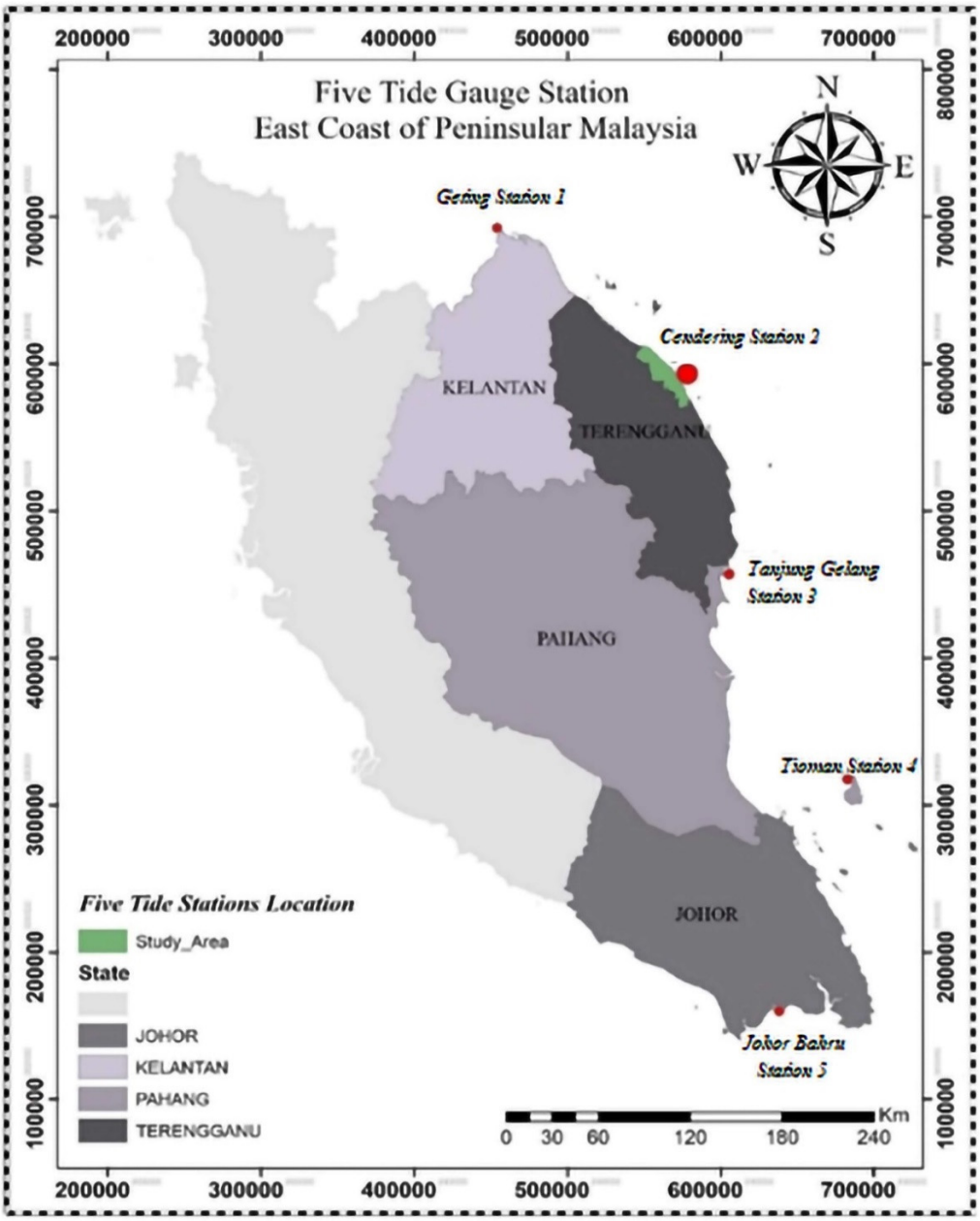

Figure 2. Tidal stations were selected for this study of sea-level rise in Terengganu, along the East Coast of Malaysia.

2.2. Time Series and Prediction Model Procedure

Figure 3 displays the methodological framework employed to address the first objective of the study. It demonstrates the necessary steps involved and the requisite data for every stage. The study distinguishes the data analysis from the application of the neural network model. Having normalized and replaced the missing data through statistical procedures, data were utilized for the training of the FNN model to ensure accurate simulation and prediction of sea levels for the East coast of Peninsular Malaysia.

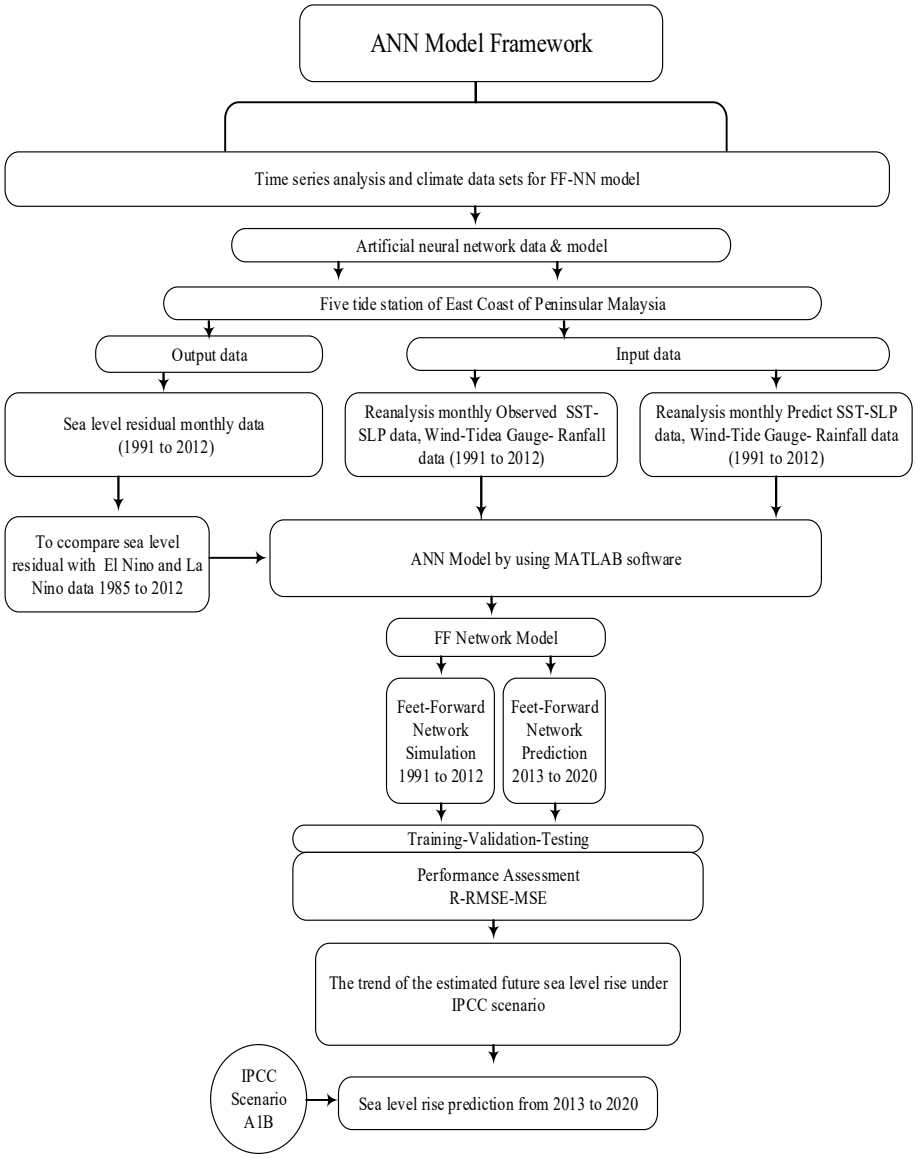

Figure 3. FNN framework for tide gauge analysis.

2.3. Field Data Collection and Data Processing

For this stage of the study, re-analysed data were used and secondary data were obtained from various sources. The main data for tide gauge, sea surface temperature, rainfall, wind, and sea level pressure was obtained from the Department of Survey and Mapping Malaysia (JUPEM). The Malaysian Meteorological Department (MMD) provided data on the monthly rainfall and monthly wind speed. Meanwhile, re-analysis data for sea surface temperature and sea level pressure were obtained from the National Centre for Environmental Prediction (NCEP).

Analysis system software from JUPEM was utilized to predict monthly tide records. The research center for the tropical climate change system at the National University of Malaysia (UKM) provided monthly anticipated rainfall data. Projections of rainfall were conducted according to the Had CM3-PRECIS climate model. The study discusses the results of the configuration and validation of the PRECIS regional climate simulation [54], while the NCEP-PCM1 provided the data on sea surface temperature and sea level pressure.

2.4. Tide Gauge Time Series Analysis and Artificial Intelligence (AI) Model

Time-series data are a series of data that are ordered chronologically [55]. The use of mean sea level data from monthly observations enables the analysis of historical records at tide stations which offers evidence of nonlinear change in sea level. This study analyses time-series sea level data (tide data) from the tide gauge stations by JUPEM collected between 1991 and 2012. Alternatively, meshless AI methods, namely ANNs, fuzzy logic, Nero-Fuzzy could be utilized to resolve the issues of near-shore sea-level change predictions. The input data were normalized to increase the efficiency of the training. Before adopting the neural network model, it is necessary to conduct a pre-treatment of the climate sample data, so the input and output data are sustainable at the steep sector of the sigmoidal transfer function, and also to increase the precision of the prediction and to strengthen the effectiveness of the data recognition [56].

It is essential to normalize output and input data to ensure that they fall within an identical range of applied transfer functions. The essence of this was to restrict their range within the interval of 0–1 [52] because the middle layer's Processing Elements (PEs) were allotted a sigmoidal activation function. Hence, this function's shape plays a vital responsibility in ANN learning. The weight variation with a value of 0 or 1 (minimal PE) is "dull," while those closer to 0.5 react more [57].

The input and target data combination was trained, validated, and tested by the ANN. The entire input and target data for executing the ANN model were normalized through Equation (1):

$$X_{normal} = 0.5 + 0.5\left(\frac{x - x_{mean}}{x_{max} - x_{min}}\right), \quad (1)$$

where X_{normal} is the normal of data, x_{mean} is the sea level residual observation mean, x_{min} is the minimum and x_{max} is the maximum sea level residual observation. Randomization of the data set will eliminate insignificant neurons with null-connection in the network output [58]. To ensure the correctness of our models, all normalized data were randomized, except the input variables for the simulation function.

2.5. Feed-Forward (FF) Model Structure

The neural network fitting tool assists in data selection, generates and trains a network, and uses regression analysis and mean square error to appraise its performance. [59] noted that the neural network can map between input datasets and a set of targets. This present study uses one of the widespread Function Fitting Neural Networks (FITNET) for the FNN model to simulate and predict changes in the sea level. In this situation, the Multilayer Perceptron (MLP) network represents the most widespread multilayer FF model.

The information in a distinctive FNN model moves only in a forward direction, from the input layer, via the hidden layers, to the output layer. The network has no loops. Each layer consists of nodes known as neurons, and each neuron in the proceeding layer is linked to other neurons. Input layer neurons only collect and forward input signals to hidden layer neurons. The other layers' neurons have the following main constituents: bias weights and an activation function that can be linear, non-linear, or continuous [52].

Mathematically, the following expressions can be used to define a neuron:

$$\nu = \sum_{i=1}^{n} w_i x_i - w_{n+1} = W.X^T - w_{n+1}, \quad (2)$$

$$y = \Psi(\nu), \tag{3}$$

where
ν = sum of all relevant products of weights and outputs from the previous layer i.
y = activation of the node at hand.
$w = [w_1, w_2, \ldots, w_n]$ vector of weights;
$x = [x_1, x_2, \ldots, x_n]$ vector of input signals;
w_{n+1} bias;
$\Psi(\nu)$ activation function;
n = Neuron number.

2.6. Evaluation and Performance Assessment

The performance assessment of prediction error explains the validation between the observed and predicted or simulated data. To select the superior neural network design that provides the most accurate and reliable simulated or forecast data, it is necessary to evaluate the findings from a time series analysis and the correctness of the ANN model [60]. To test for the accuracy of the findings of the time series analysis and the ANN model, many different types of performance measures are used. We offer the Root Mean Square Error (RMSE), Mean Absolute Error (MAE), Coefficient of Determination (R), Total Squared Error (SSE), and Mean Square Error (MSE) that provide insights into the estimation capabilities of the model [61,62].

RMSE, MAE, R, SSE, MSE are defined as follows:

$$R = \frac{\sum_{i=1}^{n}(O_i - \overline{O})(P_i - \overline{P})}{\sqrt{\sum_{i=1}^{n}(O_i - \overline{O})^2}\sqrt{\sum_{i=1}^{n}(P_i - \overline{P})^2}}, \tag{4}$$

$$MSE = \frac{1}{n}\sum_{i=1}^{n}(O_i - P_i)^2, \tag{5}$$

$$RMSE = \sqrt{\frac{1}{N}\sum_{i=1}^{n}(O_i - P_i)^2}, \tag{6}$$

$$MAE = \frac{1}{n}\sum_{i=1}^{n}|O_i - P_i|, \tag{7}$$

$$SSE = \sum_{i=1}^{n}(O_i - \overline{O}_i)^2, \tag{8}$$

where n represents the number of samples, O_i represents the observed sea level residual, P_i, represents the predicted sea level residual, $\overline{O}$ represents the mean of observed values, and $\overline{P}$ represents the mean of predicted values.

3. Results

3.1. Analysis of Relative Sea-Level Variation and Rate

The time series of the monthly tidal sea level anomaly is plotted to interpret the long-term trend of the sea level at the tide gauge stations (Figure 4). Before calculating the sea level residual to simulate and predict sea levels, outliers and missing data must be identified in the observed tide data. We performed a visual investigation using a box plot, histogram, and a Quantile-Quantile (Q-Q) to test for normal distribution and detect outliers in the time series data.

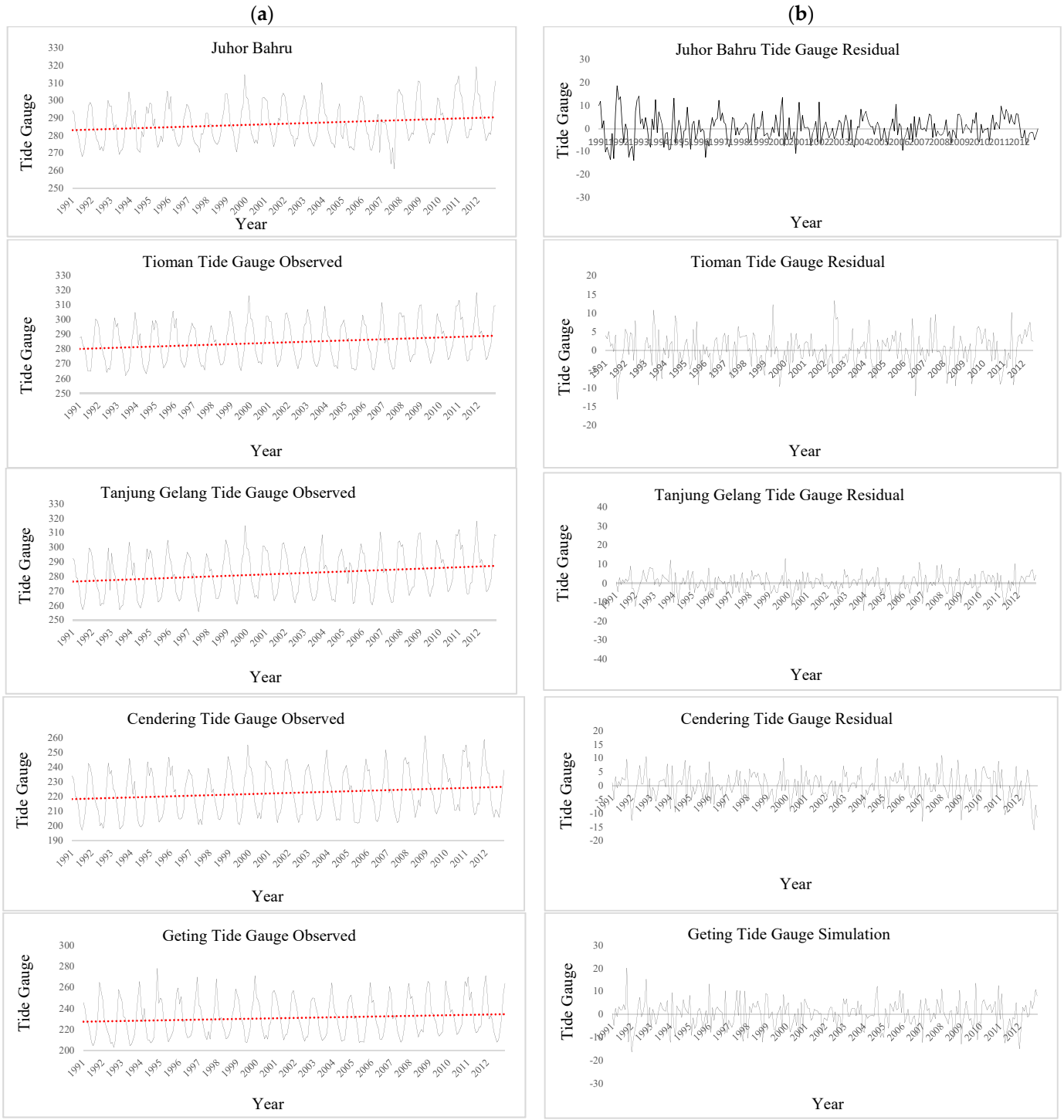

Figure 4. (**a**) Monthly tidal gauge data from five tide gauge stations between 1991 and (**b**) From 1991 to 2012, sea level residuals at five tide gauge stations along Peninsular Malaysia's East Coast.

This study used smoothing analysis and selected some statistical models to replace the missing time series data. It utilized the Holt–Winters model with R, RMSE, MAE, SSE, and MSE to obtain missing values of tide gauge data for all tide gauge stations (Table 1). It replaced the missing tide gauge data for the years 1985, 1986, 1992–1994, 1996, 1999, 2004, 2008 to 2010, and 2012 for all stations.

Table 1. The Holt–Winters performance of five tide gauge stations East Coasts of Peninsular Malaysia.

Tide Stations	RMSE	MAE	MSE	SSE	R
Juhor Bahru	0.067	0.013	0.005	0.002	0.66
Tioman	0.050	0.049	0.003	0.017	0.87
Tanjung Gelang	0.086	0.056	0.004	0.023	0.70
Cendering	0.056	0.085	0.010	0.058	0.88
Geting	0.068	0.040	0.002	0.015	0.86

The Tide Gauge Processing System (TGPS) model was applied and monthly data of tide gauges were simulated and predicted in the JUPEM software to estimate the sea level residuals. The sea level residuals are calculated as the observed minus the predicted data. The ANN model used the sea level residual data without a pattern as output data. The initial (observed) monthly tide gauge data are presented in Figure 4a, while sea level residuals are shown in Figure 4b.

A higher sea surface temperature and a lower sea level pressure would lead to higher sea level residuals and vice versa. This is probably due to the expansion of seawater due to higher temperatures. Furthermore, higher pressure exerts more force against seawater, thereby causing the surface level to be lower than the low-pressure level. Figure 5 indicates that the lowest (most negative) sea level residual was found during the La Niña event in the years 1985 to 1989, 2000, 2002, 2006, 2007, 2009, and 2011. The highest sea-level residual was associated with the El Niño event during the years 1986 to 1992, 1993, 1995, 1998, 1999, 2000, 2001, 2003, 2005, 2009, and 2011 (Figure 5).

3.2. F-ANN Model Architecture and Performance

This section presents the simulated and predicted results for sea level based on the FNN model, and it uses five input data, and one target (monthly sea level residual data from 1991 to 2020) obtained from the five tide gauge stations. The observed tide data were utilized to simulate tide gauges with the aid of the tide analysis software System JUPEM in 2012. Thus, sea level residual was the target output. Similarly, the input used for simulation and prediction were the observed monthly tide gauge data, wind, rainfall [53], sea surface temperature, and sea level pressure from 1991 to 2012. To predict sea-level change between 2013 and 2020, we applied five inputs. These data were somewhat limited, so we chose input data from 2013 to 2020. After selecting the best neural network architecture, we also chose predicted data from 2013 to 2020 and one target (output), the monthly predicted sea level residual (Figure 6). We used the neural network toolbox in MATLAB (version R2013A). The performance criteria of RMSE, MAE, R, SSE, and MSE were used to evaluate the results and conduct a quantitative assessment of the model. The formulas are given in the Section 2.

3.3. Simulation of the Model

For the FNN Model, we applied three interconnected neural network layers consisting of an input layer, a hidden layer, and an output layer. The best FNN architecture was selected after 200 runs of simulation and prediction of each tide gauge station. Thus, there are five input nodes and one output node. In hidden and output layers, each input is multiplied by a corresponding weight. The sum of the product is then calculated and processed using a function: The standard activation function comprises a linear transfer function (purelin) and a non-linear tan-sigmoid transfer function (logsig, tansig). All neurons of a particular layer usually have similar activation functions [63]. Figure 7 presents the architectures of all developed FNN model.

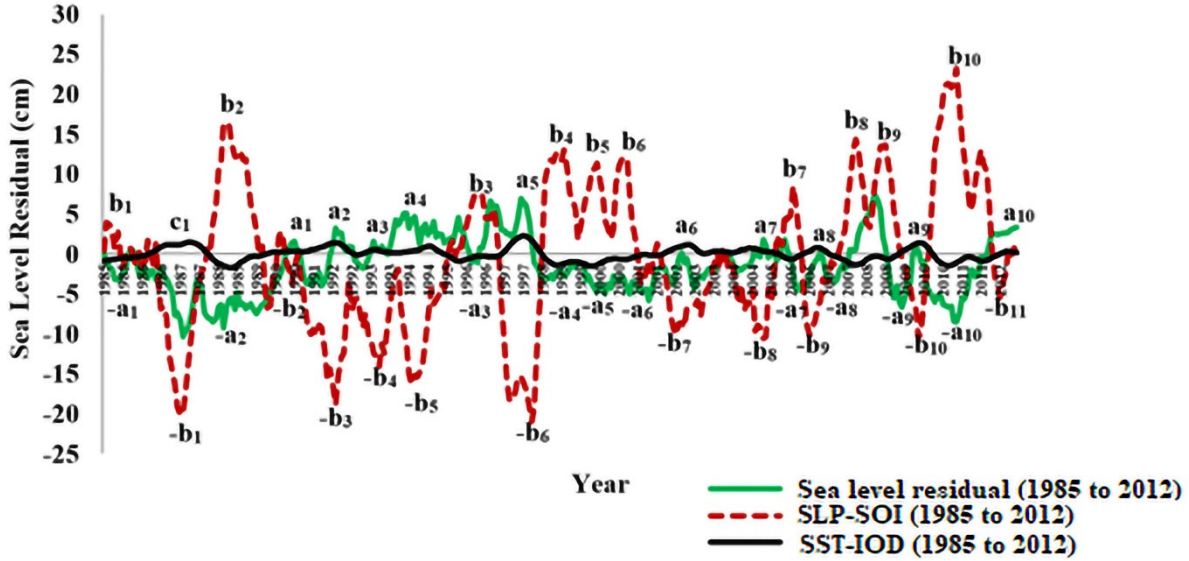

Climate data	Year																			
	1985	1987	1989	1990	1992	1993	1994	1996	1997	2000	2001	2002	2004	2006	2007	2008	2009	2010	2011	2012
HSLR (+a)				a_1	a_2	a_3	a_4		a_5			a_6	a_7		a_8			a_9		a_{10}
LSLR (−a)	$-a_1$		$-a_2$					$-a_3$		$-a_5$	$-a_6$			$-a_7$		$-a_8$	$-a_9$		$-a_{10}$	
HSLP (+b)	b_1		b_2					b_3		b_5	b_6			b_7		b_8	b_9		b_{10}	
LSLP (−b)		$-b_1$		$-b_2$	$-b_3$	$-b_4$	$-b_5$		$-b_6$			$-b_7$	$-b_8$		$-b_9$			$-b_{10}$		$-b_{11}$
HSST (+c)		C_1																		
LSST (−c)																				

Figure 5. Sea-level residuals compared between the lowest and highest El Niño and La Niño year, 1985 to 2012, of Cendering station: +a High Sea Level Residual (HSLR); −a Low Sea Level Residual (LSLR); +b High Sea Level Pressure (HSLP); −b Low Sea Level Pressure (LSLP); +c High Sea Surface Temperature (HSST), and −c Low Sea Surface Temperature (HSST).

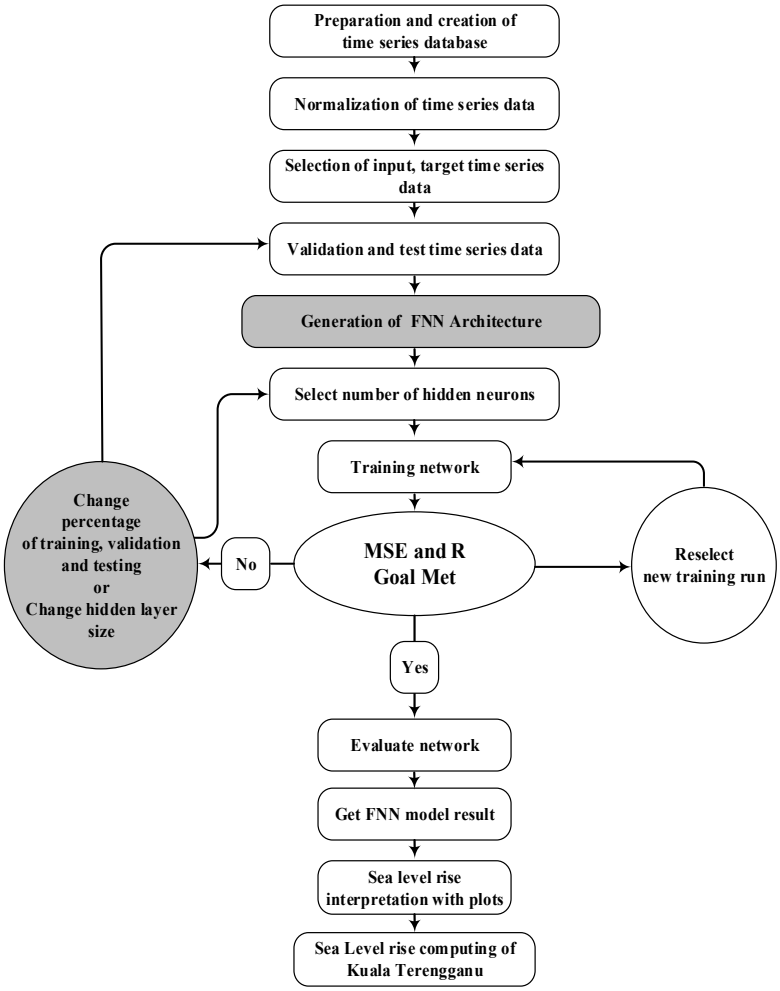

Figure 6. Flowchart of sea-level rise simulation and prediction using a Feed-Forward Neural Network model.

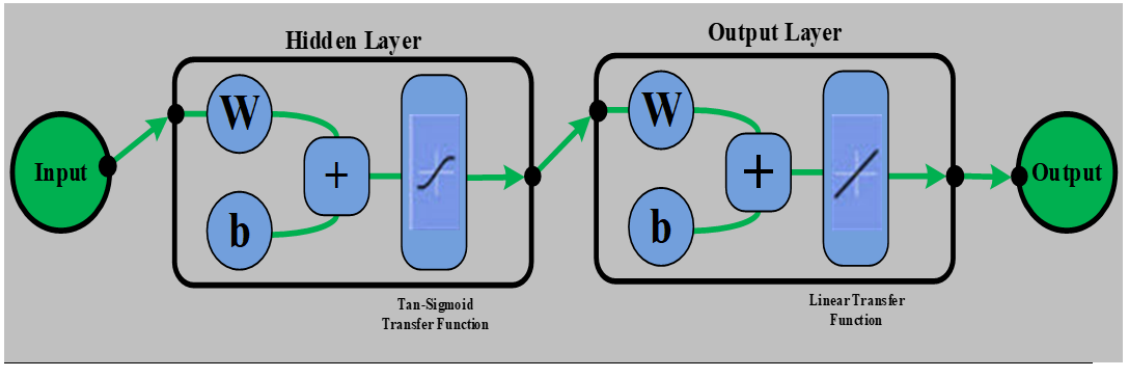

Station	FNN models: architecture (neurons in the input, hidden, and output layers)	
	Simulation model	Forecast model
Johor Bahru	5:10:1	5:10:1
Tioman	5:2:1	5:2:1
Tanjung Glang	5:5:1	5:5:1
Cendering	5:4:1	5:4:1
Geting	5:7:1	5:7:1

Figure 7. The architecture of the FNN model.

In this model, data were used for training (60%), validation (20%), and testing sets (20%), respectively. After training and running the model, the model was run 200 times. The best performance obtained from five inputs (predicted tide gauge, rainfall, sea level pressure, sea surface temperature, and wind), hidden layers (different hidden layers for each station), and one output layer were applied to determine sea-level rise via the FNN Model (Figure 7). The best simulation (1991 to 2012) and prediction (2013 to 2020) were selected with MSE and R for training, validation, and testing, respectively, (Table 2) and (Figure 8).

Table 2. The simulation performance of the FNN model.

Tide Stations	Training		Validation		Testing	
	R (%)	MSE	R (%)	MSE	R (%)	MSE
Johor Bahru (JB)	1	1.667	0.999	1.447	1	1.401
Tioman (T)	0.999	1.873	0.999	1.446	1	1.067
Tanjung Glang (TG)	0.999	1.763	0.999	1.786	0.999	1.659
Cendering (C)	1	1.277	1	1.366	0.999	1.526
Geting (G)	1	1.002	1	1.032	1	1.312

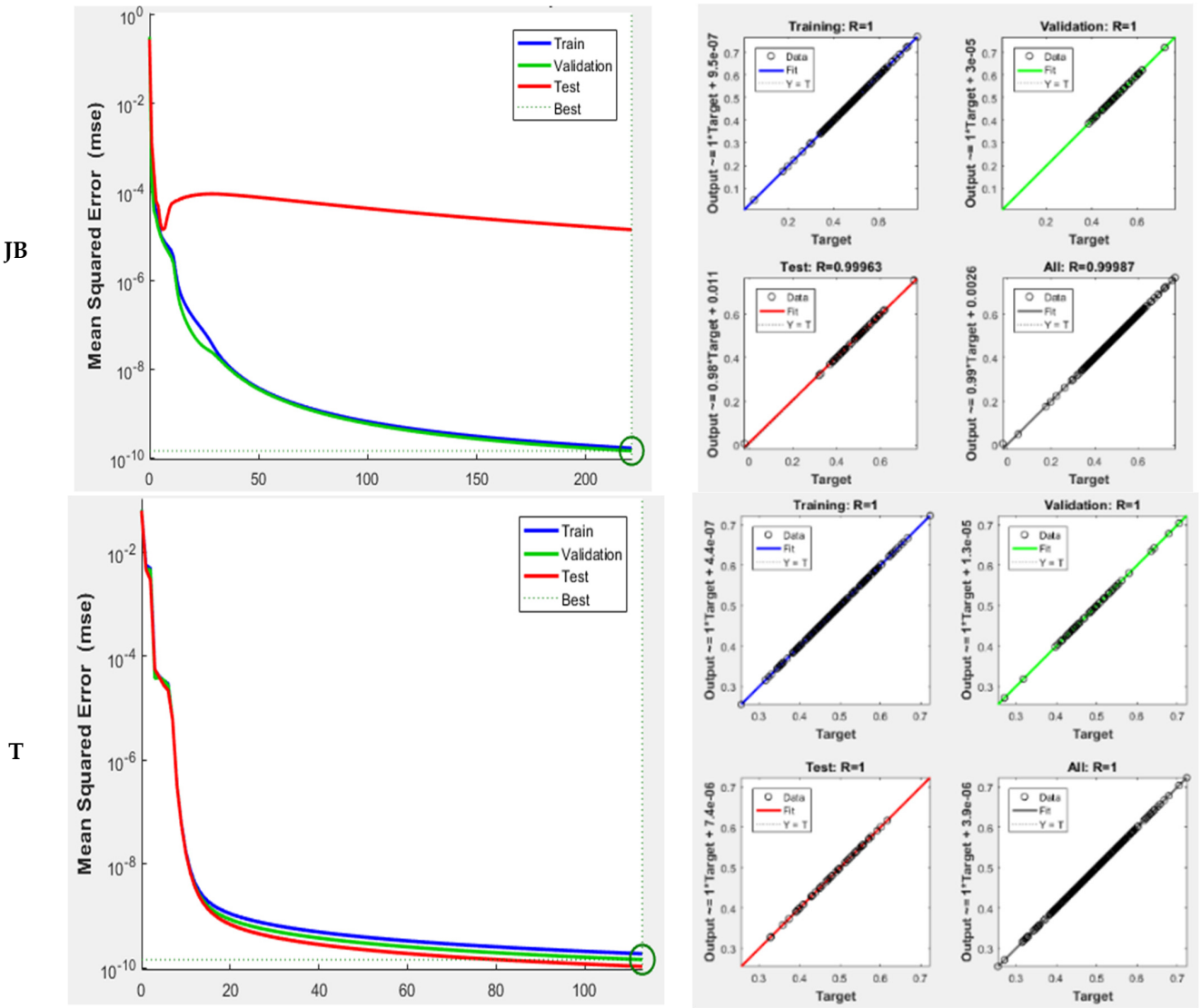

Figure 8. *Cont.*

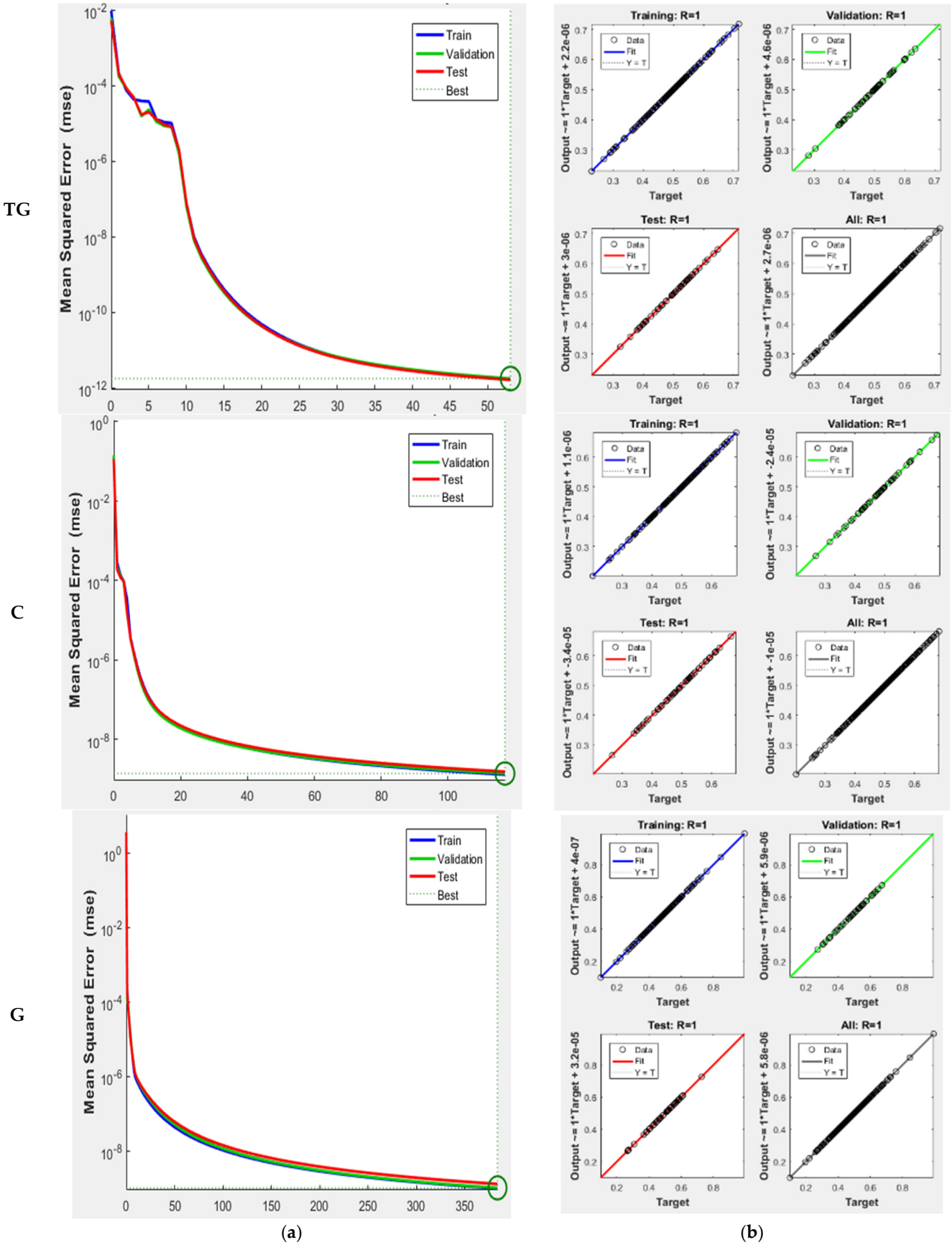

(**a**) (**b**)

Figure 8. (**a**) The model performances and (**b**) simulation validation trend from 1991 to 2012.

In Figure 8a, the blue, green, and red lines show the training, validation, and testing sets, respectively. The dotted line indicates the best performance under a minimum error. Based on the result, the best validation performance occurs at epoch 117. While due to some outliers, the FNN model at Cendering station yielded R: 1 and MSE: 1.366; the scatter plot indicates that the calculation and performance of the model are significant. The high degree of agreement between the amount observed and the simulated data from the model FNN is shown in Figure 8. This presents the plot of the sea level at Cendering and Geting stations, which is visible from R:1 and MSE:1.366 and R:1 and MSE:1.032, respectively. Figure 8b demonstrates high accuracy for the estimate by the Geting Station FNN model for which R: 1 and MSE: 1.032 were obtained. The plot of the sea level yielded by the FNN model at Cendering station (Figure 8) indicates appropriate levels of validity precision (R: 1 and MSE = 1.366). The RMSE, MAE, and SSE suggest appropriate levels of validity precision for estimates at all stations based on the FNN model. Table 2, as well as Figure 8, summarise these parameters for the FNN model. Notably, estimates at Chendering and Geting stations are superior to those obtained for the Tioman, Tanjung Gelang, and Johor Bahru stations.

3.4. Prediction of the Model

As evident from the plots in Figure 9, the FNN model yielded very strong results. The quantitative parameters R: 1 and MSE: 1.008 at Cendering station and Tanjung Glang (TG), R: 1, and MSE: 1.214 at Tanjung Glang station were returned by the FNN model. The FNN model was unable to correctly forecast sea levels at Johor Bahru station, as evidenced by some strongly over-predicted and under-predicted sea levels (Figure 9). R: 99.9 and MSE: 1.582 suggest lower forecast precision. The plot of the sea level at Geting Station shown in Figure 9 appears acceptable, but the FNN model's R: 99.9 and MSE: 1.973 still suggest a comparatively weak outlook. Table 3 presents the values of the mathematical evaluation parameters for the prediction of sea levels at all stations according to the FNN model. Based on Figure 9a, the best performance and validation with the minimum error was found at epoch 104. Figure 9b shows the result of the FNN model prediction. It indicates that the sea level change is expected to have an upward trend across 2013–2020.

Table 3. The prediction performance of the FNN model.

Tide Stations	Training		Validation		Testing	
	R (%)	MSE	R (%)	MSE	R (%)	MSE
Johor Bahru (JB)	99.9	1.953	99.9	1.585	99.4	1.517
Tioman (T)	99.9	1.617	1	1.299	1	1.052
Tanjung Glang (TG)	99.9	1.863	1	1.214	99.9	1.164
Cendering (C)	1	1.294	1	1.008	99.9	1.614
Geting (G)	1	1.570	99.9	1.973	1	1.072

Across the entire time series, the east coast Peninsular monthly sea-level rise average is at 4.60 mm/year over 29 years of tidal data collection (1991 to 2020), when averaging across all five tide gauge stations. Sea level rates at Johor Bahru in the south of Peninsular Malaysia average at 4.79 mm/year. Tioman tide gauge stations, Pahang state in the southeast region of Peninsular Malaysia, on the other hand, have a value with a rate of 4.24 mm/year. Sea level rates in Tanjung Gelang, Pahang state, averaged 4.60 mm/year during seven years (2013 to 2020). The tide gauge station at Cendering station, Kuala Terengganu city, Trengganu state in the northeast of Peninsular Malaysia displays the value with an average rate of 4.48 mm/year. At Geting station, Klantan state, in the south of Peninsular Malaysia, the average is 4.89 mm/year (Table 4).

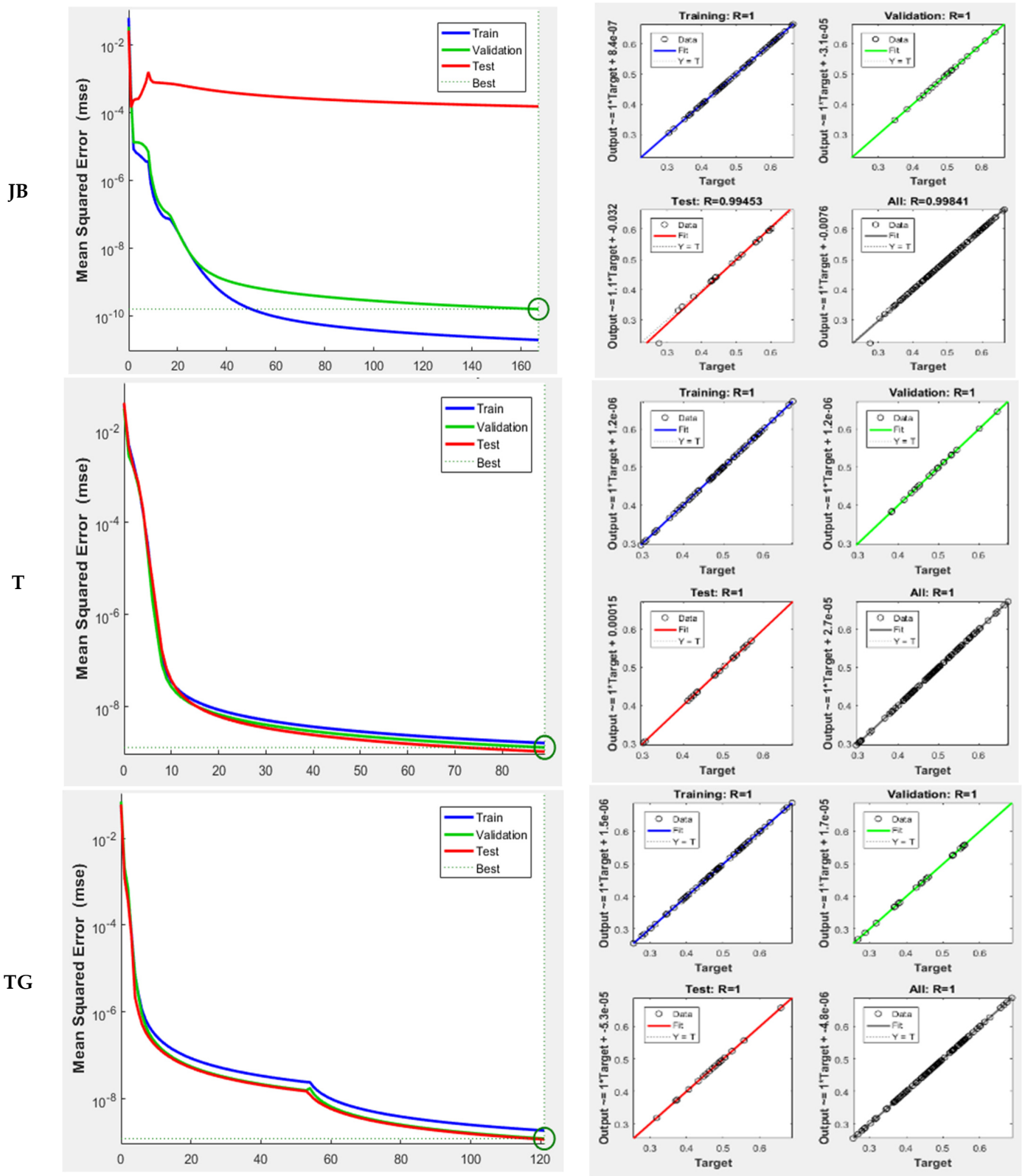

Figure 9. *Cont.*

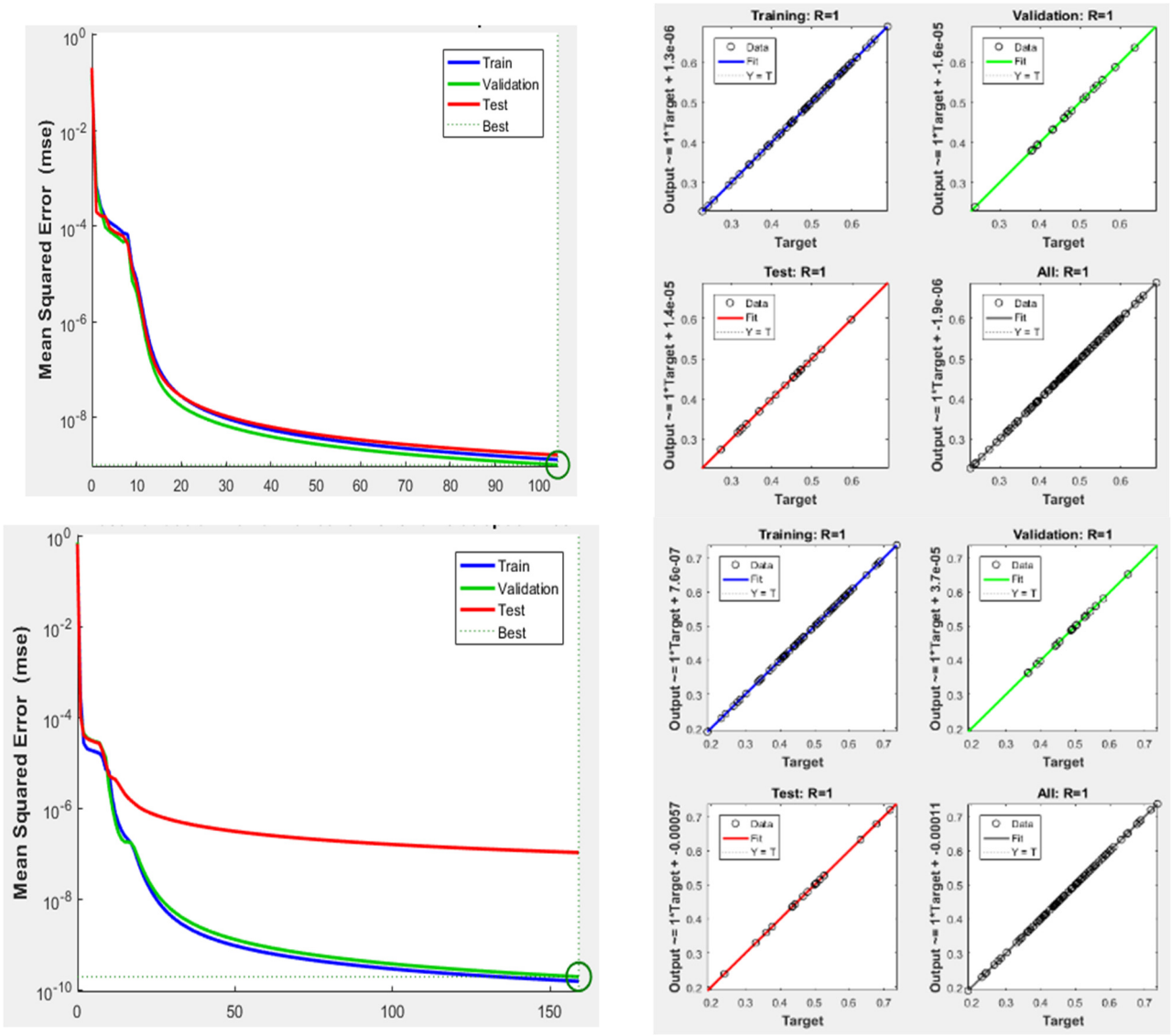

Figure 9. The model performances (**a**) and prediction validation trend (**b**) from 2013 to 2020.

Table 4. Prediction sea-level rates (mm/year) from tide gauge stations around the East Coast of Peninsular Malaysia.

Location			Start	End	Rate (mm/yr)
East Coast	L	Johor Bahru	January 2013	December 2020	2.59 ± 7.00
		Tioman	January 2013	December 2020	1.95 ± 6.54
	H	Tanjung Gelang	January 2013	December 2020	1.87 ± 7.33
		Cendering	January 2013	December 2020	1.38 ± 7.59
		Geting	January 2013	December 2020	2.46 ± 7.33

Sea level in this area varies monthly due to the tidal dynamics in this area, as there is an interchange between the Western semi-diurnal regime and the Eastern diurnal regime [63,64]. All tide gauge stations on the East coast show a greater difference in tidal scale than those on the West coast (Figure 4). In addition, more of their major diurnal components are prevalent [65,66].

The relative sea-level trend along the East coast of Peninsular Malaysia shows a linear pattern (Figure 4 and Table 1). The trends differ considerably from one location to another

and the rates of the changes in the monthly tidal data are positive, indicating an overall rise in the relative sea level.

4. Discussion

4.1. FNN Model Sea Level Predictions

Sea-level predictions hold great value for coastal areas vulnerable to coastal and shoreline changes. Following a time series data analysis, we reported the sea-level fluctuations at five gauge stations along Peninsular Malaysia's east coast, as simulated (1991 to 2012) and forecasted (2013 to 2020) using an FNN model. Figure 10 presents the simulated and predicted sea-level change data from 1991 to 2020 and their upward trend.

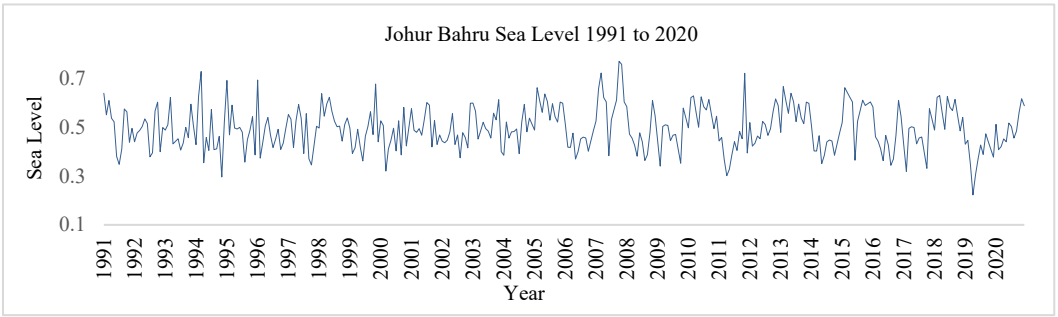

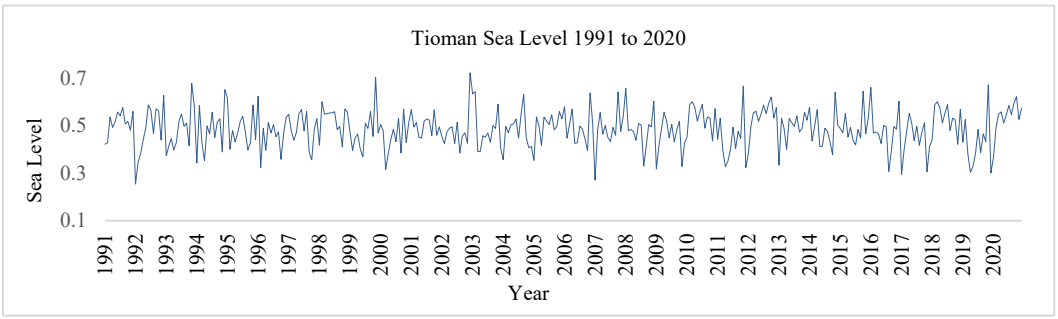

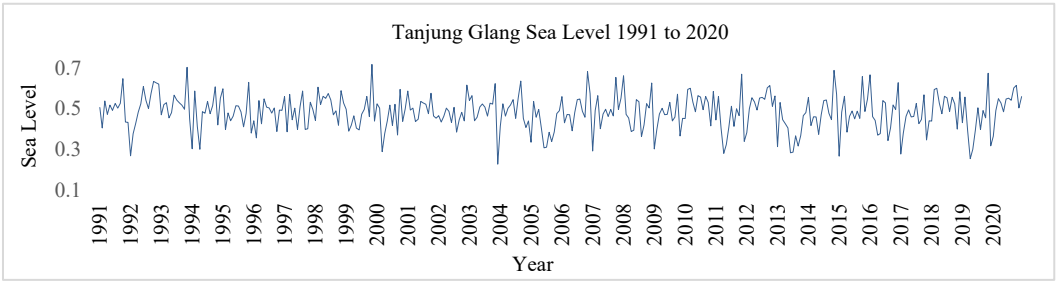

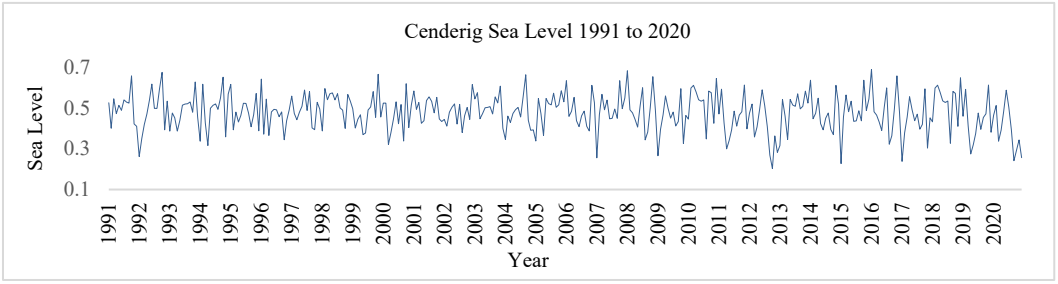

Figure 10. *Cont.*

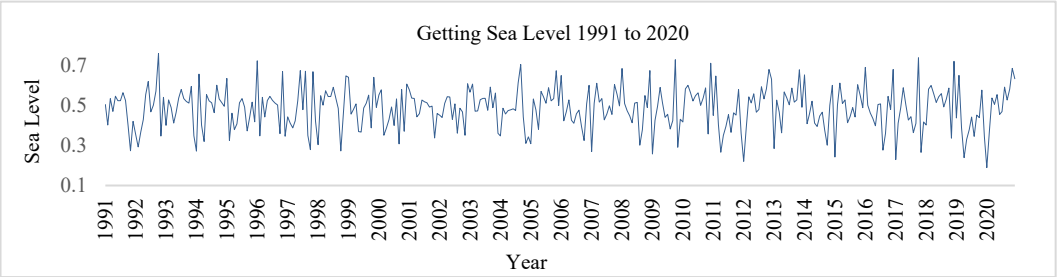

Figure 10. Sea level simulation and prediction for five tide gauge stations (1991 to 2020) located in Terengganu, along the East Coast of Malaysia.

Five different variables, namely, tidal data, wind, rainfall, sea surface temperature, and sea level pressure, were selected as inputs. They were used as predictors of sea-level change due to the high dependency on tidal gauge and climatic signal variations. Weights of the factors and the FNN model were computed in MATLAB.

4.2. Tide Gauge Results of Five Stations on the East Coast of Peninsular of Malaysia

In coastal locations subject to sea level increases, sea level prediction is a critical concern. Flooding and inundation along Malaysia's East coast could cause catastrophic harm to low-lying areas with significant populations and substantial economic activity. Johor Bahru in the south of Peninsular Malaysia has a value with a rate of 2.59 ± 7.00 mm/year. Some villages in Johor Bahru are threatened by rising sea levels. Agricultural, residential, farming and aquaculture, industrial, commerce, and services are the primary activities of this area, according to certain studies. This region, which has a high sensitivity to sea-level rise, has a lot of oil palm plantations as its land use. It should also be highlighted that the land usage of the region is the primary source of income for those in the area who depend on the oil palm plantation's output. Tioman and Tanjung Gelang tidal gauge stations in Pahang state, east peninsular Malaysia, had readings of 1.95 ± 6.54 mm/year and 1.87 ± 7.33 mm/year, respectively. The eco-tourism sector has made significant contributions to the economics and socioeconomic prosperity of Sungai Karang, a seaside city in Pahang state. Simultaneously, this behavior may have negative environmental consequences such as sea-level rise, flooding, and coastal erosion.

While there have been numerous interventions to date, the planned and strategies used to safeguard the regional-scale coastal change research conducted in Sungai Karang revealed that the government has managed to protect the coastal city area while designing various strategies for fostering the growth of eco-tourism. This might be attributed to the mainland's effectiveness in managing economic expansion and urban sprawl through its protection strategy. Further investigation is required to assess the effects of tide gauge and sea-level changes made at Tanjung Gelang station on a local scale. The rate is 1.38 ± 7.59 mm/year at the Cendering tide gauge station in Peninsular Malaysia's northeast area. The tidal gauge stations at Geting, Tanjung Gelang, and Cendering, according to the FNN model, are the most vulnerable coastal zones along Peninsular Malaysia's east coast. The Kuala Terengganu coastal city is predicted to face the most coastline alteration from Merang Kecil to UMT (Universiti Malaysia Terengganu).

Tourist destinations and industrial zones, as well as urban villages in these areas, would be among the most severely impacted economic assets. Agricultural fields, on the other hand, are often located at higher altitudes and are less likely to be exposed to such a risk. The value of a tide gauge station in the north part of Peninsular Malaysia is 2.46 ± 7.33. Recent events show that the water level is increasing along Peninsular Malaysia's east coast. From 1991 to 2020, the East Coast of Peninsular Malaysia seas has been increasing due to a high level of trust in the data and the use of the best methodologies for predicting the data. The overall significant rising sea level for the East coast of Peninsular Malaysia seas appears to be slightly lower than the rate of sea-level rise explained by a strong El

Niño event, which appears to have slowed the rate of sea-level rise along the East coast of Peninsular Malaysia seas.

This is new knowledge as there is currently insufficient information available on rates of sea-level rise. Such knowledge will enhance the capacity of planning agencies and local authorities to evaluate the effects of climate change on shorelines and coastal areas. It may further assist with planning development and land use depending on the suitability and vulnerability of specific areas in the East Coast Peninsular Malaysia. However, improved models are needed for longer-term coastal changes, including shoreline response to sea-level rise and potential human adaptations like beach nourishment. The long-term evolution of sandy coastal areas, including the role of sea-level rise, is another important area of study. This research presents the first study of five tide gauge stations in the east coast Peninsular Malaysia area. It introduces a better understanding of how to model sea-level change through mathematical and AI approaches for sandy beaches at the local level. It is a first step towards the development of digital and numerical data tools for the analysis of observed and historical sea-level positions.

4.3. Sea-Level Rise and Hazard Vulnerability

The consequences of sea-level rise and inundation events, including flooding, pose a danger to low-lying areas like the Terengganu, Pahang, and coastal zone. The climate and tidal gauge data obtained through this study can assist with establishing a web-based coastal city Geography Information System (GIS) for East Coast Economic Regine as needed for climate change-related hazard planning. Our simple and yet effective mathematical model used vertical point prediction (from the shoreline) for each tide gauge station along the East Coast of Peninsular Malaysia. It is easily implemented and conveyed to coastal planners and Malaysian government staff, which makes it a useful tool for communication. The data on sea-level fluctuations along Peninsular Malaysia's east coast is particularly useful for coastal city management, urban development, and flood control. It's also crucial to consider when estimating sea-level rise because of the implications for future regional climate. For coastal adaptation, a coastal area with projected sea-level rise information can be employed. As a result, adaptation measures are required to mitigate the potential impacts of sea-level rise, particularly in coastal areas. Adaptation strategies such as coastal defenses, beach nourishment, erosion, flood, and mangrove development, among others, should be adopted in Malaysia to prevent the harmful impact of sea-level rise.

To stabilize beaches in the areas most likely to be affected, we recommend adaptive measures such as beach replenishment, dune restoration, and hard structures to absorb wave energy. Furthermore, increasing awareness and developing appropriate policies are critical for long-term development. Our findings will inform decision-making in this context. Results of the FNN model were effective at predicting sea levels and their changing patterns, inferring from the minimum MSE, RMSE, MAS, SSD, and maximum R. The FNN model has the best performing architecture among the ANNs model. This model simulates the patterns of sea level well and can therefore be used to predict sea-level changes. Changes in sea level are associated with changes in tidal gauge and climatic variations, especially sea surface temperature and sea level pressure. There is a positive relationship between the sea surface temperature and sea level residual, while a negative relationship exists between the sea level pressure and sea level residual.

The findings of this research can also be used to plan and manage climate change-related risks of hazardous events such as erosion and floods [53]. The study employed an ANN architecture model framework for examining the impact of sea-level change, and although relatively basic data were input, the findings suggest that such work has value for coastal city planning and human use of shorelines in the future. The FNN models can support time-series data, and inputs can be changed by the researcher for different study areas. This study shows that the relative sea-level along the East Coast of Peninsular Malaysia follows a linear pattern of robust fit regression. Changes in sea-level trends, notably and sea level pressure, are linked to changes in tide gauges and climatic

fluctuations. The sea surface temperature and sea level residual of the five tide gauge stations showed a positive relationship; however,, the sea level pressure and sea level residual showed a negative relationship.

5. Conclusions

Sea-level predictions have great value for coastal cities that are sensitive to sea-level fluctuations. Here, we analyzed measurements of the sea level (tidal gauge time series data) from five tidal gauge stations along the East Coast of Peninsular Malaysia. Using an FNN model soft computing technology, increases in sea level were simulated (1991–2012) and predicted (2013–2020). Five input variables were used for the FNN model as they majorly influence sea-level change: tidal gauge, rainfall, wind, sea level pressure, and sea surface temperature. The weights of the components were calculated, and FNN modeling was performed using MATLAB. Our approach overcame numerous shortfalls of other techniques, as we discussed in detail in the Introduction.

The sea-level rise fluctuated by roughly 7.61 mm/year across the whole period in East Coast of Peninsular Malaysia, with higher readings at the tidal gauge station at Cendering in Kuala Terengganu, Terengganu state and with an average rate of 7.59 mm/year, and Tanjung Gelang, Pahang state with an average rate of 7.59 mm/year following the Cendering station. The Tioman tidal gauge station in Puala Tioman, Pahang state, had the lowest figure, with a rate of 6.54 mm/year and fluctuating monthly predicted sea-level changes. The relative sea-level rate increased along Peninsular Malaysia's east coast, ranging from 2.05 to 7.16 mm/year, with an average of 4.60 mm/year. Our findings can be used as a guideline for planning agencies and municipal councils working on coastline development and risk reduction.

The result of this study is consistent with the studies of [64,65]. Cnducted studies on how climate change affects sea-level change in Malaysia and projected sea-level rise for Peninsular Malaysia [66]. For the year 2100, this was projected to be in a range of 2.50–5.0 mm/year by the most severely affected low-lying Northeast and West coast areas of the peninsular (Kelantan and Kedah). The study revealed a significant increase in sea-level rise in the past five years, compared to 20 years ago. For the period of 1993–2010, the observed average sea level rate along the Malaysian coast was anticipated to be between 2.7 and 7.0 mm/year [11,67]. In another [68] report, about 3.3% of the 1963 km of coastline is categorized as severely vulnerable. These sites comprise the northern reaches of the Kedah shoreline and the southern stretches of the Terengganu shoreline.

As a result, these predictions might be valuable for warning about the likely high rate of sea-level changes (rise), which could have an impact on the livelihood and economics of Kuala Terengganu's coastal districts. As a result, it may lessen the impact of sea-level rise on the population and socioeconomic well-being of the country. The result may also be used to forecast future hazard events in this area, such as erosion and flooding. In the future, managers and policymakers will need to know about this conclusion. Furthermore, the research might help people involved in coastal planning, policy, and decision-making evaluate the effects of climate change on the shoreline and coastal region and produce long-term and short-term projections of land use appropriateness in coastal areas. These possible sea-level rise rates can be used as a guide for planning and implementation organisations as well as local governments in their development plans to avoid significant de-development in crucial regions.

Author Contributions: Data curation, M.B.; Formal analysis, M.B.; Funding acquisition, Z.Z.I., M.F.A. and W.I.A.W.T.; Investigation, W.I.A.W.T., B.O. and S.R.; Methodology, M.B.; Project administration, Z.Z.I. and A.B.P.; Resources, Z.Z.I., W.I.A.W.T., B.O., S.R. and I.D.W.; Software, M.B.; Validation, I.D.W.; Writing—original draft, M.B.; Writing—review & editing, M.F.A., W.I.A.W.T., B.O., S.R., I.D.W. and A.B.P. All authors have read and agreed to the published version of the manuscript.

Funding: Financial support and research facilities were provided by the Faculty of Environmental Studies, Department of Environmental Management, Universiti Putra Malaysia (UPM), Malaysia, 43400, Serdang, Selangor, Malaysia. Sources: UPM-RUGS 4: Project Number (03-04-11-1477RU)

and: UPM-RUGS 6: Project Number (03-01-12-1664RU). Also acknowledged is the INOS Higher Institution of Centre of Excellence (UMT-LRGS (56041)) for partially supporting the extension of the study.

Institutional Review Board Statement: Not applicable.

Informed Consent Statement: Not applicable.

Data Availability Statement: Not applicable.

Conflicts of Interest: The authors declare no conflict of interest.

References

1. Pessoa, M.F.; Lidon, F.C. Impact of human activities on coastal vegetation—A review. *Emir. J. Food Agric.* **2013**, *25*, 926–944. [CrossRef]
2. Jiménez, J.A.; Valdemoro, H.I.; Bosom, E.; Sánchez-Arcilla, A.; Nicholls, R.J. Impacts of sea-level rise-induced erosion on the Catalan coast. *Reg. Environ. Chang.* **2017**, *17*, 593–603. [CrossRef]
3. Folger, P.; Carter, N.T. *Sea-Level Rise and US Coasts: Science and Policy Considerations*; Congressional Research Service: Washington, DC, USA, 2016.
4. Bagheri, M.; Zaiton Ibrahim, Z.; Akhir, M.F.; Talaat, W.I.A.W.; Oryani, B.; Rezania, S.; Pour, A.B. Developing a Climate Change Vulnerability Index for Coastal City Sustainability, Mitigation, and Adaptation: A Case Study of Kuala Terengganu, Malaysia. *Land* **2021**, *10*, 1271. [CrossRef]
5. Nauels, A.; Gütschow, J.; Mengel, M.; Meinshausen, M.; Clark, P.U.; Schleussner, C.F. Attributing long-term sea-level rise to Paris Agreement emission pledges. *Proc. Natl. Acad. Sci. USA* **2019**, *116*, 23487–23492. [CrossRef] [PubMed]
6. Schneider, P.; Asch, F. Rice production and food security in Asian Mega deltas—A review on characteristics, vulnerabilities and agricultural adaptation options to cope with climate change. *J. Agron. Crop Sci.* **2020**, *206*, 491–503. [CrossRef]
7. Bagheri, M.; Zaiton Ibrahim, Z.; Mansor, S.; Abd Manaf, L.; Akhir, M.F.; Talaat, W.I.A.W.; Beiranvand Pour, A. Application of Multi-Criteria Decision-Making Model and Expert Choice Software for Coastal City Vulnerability Evaluation. *Urban. Sci.* **2021**, *5*, 84. [CrossRef]
8. Mimura, N. Sea-level rise is caused by climate change and its implications for society. *Proc. Jpn. Acad. Ser. B* **2013**, *89*, 281–301. [CrossRef]
9. Kamruzzaman, M.; Jang, M.W.; Cho, J.; Hwang, S. Future Changes in Precipitation and Drought Characteristics over Bangladesh under CMIP5 Climatological Projections. *Water* **2019**, *11*, 2219. [CrossRef]
10. IPCC. *Climate Change 2014: Synthesis Report*; Pachauri, R.K., Meyer, L.A., Eds.; Contribution of Working Groups I, II, and III to the Fifth Assessment Report of the Intergovernmental Panel on Climate Change; IPCC: Geneva, Switzerland, 2014; p. 151.
11. Meier, M.F.; Wahr, J.M. Sea level is rising: Do we know why? *Proc. Natl. Acad. Sci. USA* **2002**, *99*, 6524–6526. [CrossRef] [PubMed]
12. Clark, P.U.; Church, J.A.; Gregory, J.M.; Payne, A.J. Recent progress in understanding and projecting regional and global mean sea-level change. *Curr. Clim. Chang. Rep.* **2015**, *1*, 224–246. [CrossRef]
13. Rezania, S.; Oryani, B.; Cho, J.; Sabbagh, F.; Rupani, P.F.; Talaiekhozani, A.; Rahimi, N.; Lotfi Ghahroud, M. Technical Aspects of Biofuel Production from Different Sources in Malaysia—A Review. *Processes* **2020**, *8*, 993. [CrossRef]
14. Shaffril, H.A.M.; Abu Samah, B.; D'Silva, J.L.; Jegak, U. Global warming at the east coast zone of Peninsular Malaysia. *Am. J. Agric. Biol. Sci.* **2011**, *6*, 377–383. [CrossRef]
15. Awang, N.A.; Hamid, M.R.A. Sea level rise in Malaysia. Sea level rise adaptation measures. *Hydrolink* **2013**, *2*, 47–49.
16. Cabral, H.; Fonseca, V.; Sousa, T.; Costa Leal, M. Synergistic effects of climate change and marine pollution: An overlooked interaction in coastal and estuarine areas. *Int. J. Environ. Res. Public Health* **2019**, *16*, 2737. [CrossRef]
17. Ariffin, E.H.; Sedrati, M.; Akhir, M.F.; Norzilah, M.N.M.; Yaacob, R.; Husain, M.L. Short-term observations of beach Morphodynamics during seasonal monsoons: Two examples from Kuala Terengganu coast (Malaysia). *J. Coast. Conserv.* **2019**, *23*, 985–994. [CrossRef]
18. Din, A.H.M.; Hamid, A.I.A.; Yazid, N.M.; Tugi, A.; Khalid, N.F.; Omar, K.M.; Ahmad, A. Malaysian Sea Water Level Pattern Derived from 19 Years Tidal Data. *J. Teknol.* **2017**, *79*, 137–145. [CrossRef]
19. Foster, G.; Brown, P.T. Time and tide: Analysis of sea level time series. *Clim. Dyn.* **2015**, *45*, 291–308. [CrossRef]
20. Beenstock, M.; Felsenstein, D.; Frank, E.; Reingewertz, Y. Tide gauge location and the measurement of global sea-level rise. *Environ. Ecol. Stat.* **2015**, *22*, 179–206. [CrossRef]
21. Bradshaw, E.; Rickards, L.; Aarup, T. Sea level data archaeology and the global sea level observing system (GLOSS). *GeoResJ* **2015**, *6*, 9–16. [CrossRef]
22. Wöppelmann, G.; Pirazzoli, P.A. Tide Gauges. In *Encyclopedia of Coastal Science*; Schwartz, M.L., Ed.; Encyclopedia of Earth Science Series; Springer: Dordrecht, The Netherlands, 2005. [CrossRef]
23. Buonocore, B.; Cotroneo, Y.; Capozzi, V.; Aulicino, G.; Zambardino, G.; Budillon, G. Sea-Level Variability in the Gulf of Naples and the "Acqua Alta" Episodes in Ischia from Tide-Gauge Observations in the Period 2002–2019. *Water* **2020**, *12*, 2466. [CrossRef]
24. Johari, A.; Akhir, M.F. Exploring thermocline and water masses variability in the southern South China Sea from the World Ocean Database (WOD). *Acta Oceanol. Sin.* **2019**, *38*, 38–47. [CrossRef]

25. Din, A.H.M.; Abazu, I.C.; Pa'suya, M.F.; Omar, K.M.; Hamid, A.I.A. The impact of sea-level rise on geodetic vertical datum of Peninsular Malaysia. *Int. Arch. Photogramm. Remote Sens. Spat. Inf. Sci.* **2016**, *42*, 237–245. [CrossRef]
26. Garcin, M.; Baills, A.; Le Cozannet, G.; Bulteau, T.; Auboin, A.L.; Sauter, J. Pluridecadal impact of mining activities on coastline mobility of estuaries of New Caledonia (South Pacific). *J. Coast. Res.* **2013**, *65*, 494–499. [CrossRef]
27. Huang, Y. Advances in artificial neural networks–methodological development and application. *Algorithms* **2009**, *2*, 973–1007. [CrossRef]
28. Hopfield, J.J. Neural networks and physical systems with emergent collective computational abilities. *Proc. Natl. Acad. Sci. USA* **1982**, *79*, 2554–2558. [CrossRef] [PubMed]
29. Hung, N.Q.; Babel, M.S.; Weesakul, S.; Tripathi, N.K. An artificial neural network model for rainfall forecasting in Bangkok, Thailand. *Hydrol. Earth Syst. Sci. Discuss.* **2008**, *5*, 183–218. [CrossRef]
30. Abiodun, O.I.; Jantan, A.; Omolara, A.E.; Dada, K.V.; Mohamed, N.A.; Arshad, H. State-of-the-art in artificial neural network applications: A survey. *Heliyon* **2018**, *4*, e00938. [CrossRef]
31. Alaloul, W.S.; Qureshi, A.H. Data Processing Using Artificial Neural Networks. In *Dynamic Data Assimilation-Beating the Uncertainties*; IntechOpen: London, UK, 2020.
32. Catic, A.; Gurbeta, L.; Kurtovic-Kozaric, A.; Mehmedbasic, S.; Badnjevic, A. Application of Neural Networks for classification of Patau, Edwards, Down, Turner, and Klinefelter Syndrome based on first-trimester maternal serum screening data, ultrasonographic findings, and patient demographics. *BMC Med. Genom.* **2018**, *11*, 19. [CrossRef]
33. Cabaneros, S.M.; Calautit, J.K.; Hughes, B.R. A review of artificial neural network models for ambient air pollution prediction. *Environ. Model. Softw.* **2019**, *119*, 285–304. [CrossRef]
34. Changwei, Y.; Zonghao, L.; Xueyan, G.; Wenying, Y.; Jing, J.; Liang, Z. Application of BP neural network model in risk evaluation of railway construction. In *Complexity*; Hindawi: London, UK, 2019.
35. Said, M.I.M. Artificial Intelligence Approach to Predicting River Water Quality: A Review. *J. Environ. Treat. Tech.* **2020**, *8*, 1093–1100.
36. Yuan, Q.; Shen, H.; Li, T.; Li, Z.; Li, S.; Jiang, Y.; Gao, J. Deep learning in environmental remote sensing: Achievements and challenges. *Remote Sens. Env.* **2020**, *241*, 111716. [CrossRef]
37. Ouma, Y.O.; Okuk, C.O.; Njau, E.N. Use of Artificial Neural Networks and Multiple Linear Regression Model for the Prediction of Dissolved Oxygen in Rivers: Case Study of Hydrographic Basin of River Nyando, Kenya. In *Complexity*; Hindawi: London, UK, 2020.
38. Wang, Y.; Ni, X.S.; Stone, B. A two-stage hybrid model by using artificial neural networks as feature construction algorithms. *Int. J. Data Min. Knowl. Manag. Process* **2018**, *8*, 6. [CrossRef]
39. Hornik, K. Some new results on neural network approximation. *Neural Netw.* **1993**, *6*, 1069–1072. [CrossRef]
40. Haykin, S.S. *Neural Networks. A Comprehensive Foundation*; Prentice-Hall: Hamilton, ON, Canada, 1999.
41. Runge, J.; Zmeureanu, R. Forecasting energy use in buildings using artificial neural networks: A review. *Energies* **2019**, *12*, 3254. [CrossRef]
42. Bertolaccini, L.; Solli, P.; Pardolesi, A.; Pasini, A. An overview of the use of artificial neural networks in lung cancer research. *J. Thorac. Dis.* **2017**, *9*, 924. [CrossRef] [PubMed]
43. Zhao, L.; Hicks, F.E.; Fayek, A.R. Applicability of multilayer feed-forward neural networks to model the onset of river breakup. *Cold Reg. Sci. Technol.* **2012**, *70*, 32–42. [CrossRef]
44. Masters, T. *Practical Neural Network Recipes in C++*; Academic Press: Cambridge, MA, USA; Morgan Kaufmann: San Diego, CA, USA, 1993.
45. Mas, J.F.; Puig, H.; Palacio, J.L.; Sosa-López, A. Modeling deforestation using GIS and artificial neural networks. *Environ. Model. Softw.* **2004**, *19*, 461–471. [CrossRef]
46. Molinari, D.; De Bruijn, K.; Castillo, J.; Aronica, G.T.; Bouwer, L.M. Review Article: Validation of flood risk models: Current practice and innovations. *Nat. Hazards Earth Syst. Sci. Discuss.* **2017**. in review. [CrossRef]
47. Fredrick, M.H.; Kostanic, I. *Principles of Neurocomputing for Science and Engineering*; Mc Graw Hill: New York, NY, USA, 2001; ISBN 0-0-025966-6.
48. Hornik, K.; Stichcombe, M.; White, H. Multi-layer feedforward networks are universal approximators. *Neural Netw.* **1989**, *2*, 359–366. [CrossRef]
49. Eftekhar, B.; Mohammad, K.; Ardebili, H.E.; Ghodsi, M.; Ketabchi, E. Comparison of artificial neural network and logistic regression models for prediction of mortality in head trauma based on initial clinical data. *BMC Med Inform. Decis. Mak.* **2005**, *5*, 3. [CrossRef]
50. Tezel, G.; Buyukyildiz, M. Monthly evaporation forecasting using artificial neural networks and support vector machines. *Appl. Clim.* **2016**, *124*, 69–80. [CrossRef]
51. Makarynskyy, O.; Makarynska, D.; Rayson, M.; Langtry, S. Combining deterministic modeling with artificial neural networks for suspended sediment estimates. *Appl. Soft Comput.* **2015**, *35*, 247–256. [CrossRef]
52. Tasadduq, I.; Rehman, S.; Bubshait, K. Application of neural networks for the prediction of hourly mean surface temperatures in Saudi Arabia. *Renew. Energy* **2002**, *25*, 545–554. [CrossRef]
53. Bagheri, M.; Ibrahim, Z.Z.; Mansor, S.B.; Abd Manaf, L.; Badarulzaman, N.; Vaghefi, N. Shoreline change analysis and erosion prediction using historical data of Kuala Terengganu, Malaysia. *Environ. Earth Sci.* **2019**, *78*, 477. [CrossRef]

54. Polo, F.A.O.; Bermejo, J.F.; Fernández, J.F.G.; Márquez, A.C. Failure mode prediction and energy forecasting of PV plants to assist dynamic maintenance tasks by ANN-based models. *Renew. Energy* **2015**, *81*, 227–238. [CrossRef]
55. Kwan, M.S.; Tangang, F.T.; Juneng, L. Present-day regional climate simulation over Malaysia and the western Maritime Continent region using PRECIS forced with ERA40 reanalysis. *Appl. Clim.* **2014**, *115*, 1–14. [CrossRef]
56. Amerian, Y.; Voosoghi, B. Least-squares spectral analysis for detection of systematic behavior of digital level compensator. *J. Geod. Sci.* **2011**, *1*, 35–40. [CrossRef]
57. Zime, S. *Africa Economic Growth Forecasting Research Based on Artificial Neural Network Model: Case Study of Benin*; University of Electronic Science and Technology of China: Chengdu, China, 2014; Volume 3, ISSN 2278-0181.
58. Ghamarnia, H.; Jalili, Z. Artificial network for predicting water uptake under shallow saline ground water conditions. *J. Sci. Res. Rep.* **2015**, *7*, 359–372. [CrossRef]
59. Olden, J.D.; Jackson, D.A. Illuminating the "black box": A randomization approach for understanding variable contributions in artificial neural networks. *Ecol. Model.* **2002**, *154*, 135–150. [CrossRef]
60. Demuth, H.; Beale, M.; Hagan, M. *Neural Network Toolbox™ 6 User's Guide*; MathWorks: Natick, MA, USA, 1992.
61. Khamis, A.; Abdullah, S.N.S.B. Forecasting Wheat Price Using Backpropagation and NARX Neural Network. *Int. J. Eng. Sci.* **2014**, *3*, 19–26.
62. Nitsure, S.P.; Londhe, S.N.; Khare, K.C. Prediction of seawater levels using wind information and soft computing techniques. *Appl. Ocean Res.* **2014**, *47*, 344–351. [CrossRef]
63. Mashaly, A.F.; Alazba, A.A.; Al-Awaadh, A.M.; Mattar, M.A. A predictive model for assessing and optimizing solar still performance using artificial neural networks under a hyper-arid environment. *Sol. Energy* **2015**, *118*, 41–58. [CrossRef]
64. Makarynskyy, O.; Makarynska, D.; Kuhn, M.; Featherstone, W.E. Predicting sea level variations with artificial neural networks at Hillarys Boat Harbour, Western Australia. Estuarine. *Coast. Shelf Sci.* **2004**, *61*, 351–360. [CrossRef]
65. Rafiean, H.; Aliei, M. Application of Neuro-Fuzzy Model for Predicting Sea Level Rise Utilizing Climatic Signals: A Case Study. *Tech. J. Eng. Appl. Sci.* **2013**, *3*, 3825–3830.
66. NAHRIM. *The Study of the Impact of Climate Change on Sea-Level Rise in Malaysia (Final Report)*; National Hydraulic Research Institute Malaysia: Seri Kembangan, Malaysia, 2010; p. 172.
67. Din, A.H.M.; Zulkifli, N.A.; Hamden, M.H.; Aris, W.A.W. Sea level trend over Malaysian seas from multi-mission satellite altimetry and vertical land motion-corrected tidal data. *Adv. Space Res.* **2019**, *63*, 3452–3472. [CrossRef]
68. NAHRIM. *Proceedings of the National Seminar on Coastal Morphology (COSMO) on the Muddy Coast of Malaysia (Final Report)*; Coastal Research Centre, National Hydraulic Research Institute Malaysia (NAHRIM): Seri Kembangan, Malaysia, 2010; p. 220.